

ELECTRON-ION RECOMBINATION MEASUREMENTS MOTIVATED BY AGN X-RAY ABSORPTION FEATURES: FE XIV FORMING FE XIII

E. W. SCHMIDT,¹ S. SCHIPPERS,¹ A. MÜLLER,¹ M. LESTINSKY,² F. SPRENGER,² M. GRIESER,² R. REPNOW,² A. WOLF,² C. BRANDAU,^{3,1} D. LUKIĆ,⁴ M. SCHNELL,⁴ AND D. W. SAVIN⁴

Draft version March 20, 2022

ABSTRACT

Recent spectroscopic models of active galactic nuclei (AGN) have indicated that the recommended electron-ion recombination rate coefficients for iron ions with partially filled M-shells are incorrect in the temperature range where these ions form in photoionized plasmas. We have investigated this experimentally for Fe XIV forming Fe XIII. The recombination rate coefficient was measured employing the electron-ion merged beams method at the Heidelberg heavy-ion storage-ring TSR. The measured energy range of 0–260 eV encompassed all dielectronic recombination (DR) $1s^2 2s^2 2p^6 3l 3l' 3l'' nl''''$ resonances associated with the $3p_{1/2} \rightarrow 3p_{3/2}$, $3s \rightarrow 3p$, $3p \rightarrow 3d$ and $3s \rightarrow 3d$ core excitations within the M-shell of the Fe XIV ($1s^2 2s^2 2p^6 3s^2 3p$) parent ion. This range also includes the $1s^2 2s^2 2p^6 3l 3l' 4l'' nl''''$ resonances associated with $3s \rightarrow 4l''$ and $3p \rightarrow 4l''$ core excitations. We find that in the temperature range 2–14 eV, where Fe XIV is expected to form in a photoionized plasma, the Fe XIV recombination rate coefficient is orders of magnitude larger than previously calculated values.

Subject headings: atomic data — atomic processes — plasmas — galaxies: active — galaxies: nuclei — X-rays: galaxies

1. INTRODUCTION

Recent spectroscopic XMM-Newton and Chandra X-ray observations of active galactic nuclei (AGN) have detected a new absorption feature around 15–17 Å (Sako et al. 2001; Pounds et al. 2001; Kaspi et al. 2002; Behar et al. 2003; Steenbrugge et al. 2003; Kaspi et al. 2004; Gallo et al. 2004; Pounds et al. 2004; Krongold et al. 2005). This has been identified as an unresolved transition array (UTA) due mainly to $2p \rightarrow 3d$ inner shell absorption in moderately charged iron ions with an open M-shell (Fe I–Fe XVI). On the basis of atomic structure calculations and photoabsorption modeling, Behar, Sako, & Kahn (2001) pointed out that the shape of the UTA features can be used for diagnostics of the AGN absorber. However, Netzer et al. (2003) noted a disagreement between the predicted and observed shape of this feature. As a possible cause for this discrepancy they suggested an underestimation of the low temperature dielectronic recombination (DR) rate coefficients for iron M-shell ions. These rate coefficients determine the charge state balance of the iron M-shell ions in a photoionized plasma and, consequently, the shape of the UTA.

Reliable low temperature DR rate coefficients of iron M-shell ions are not available in the literature. The widely used compilation of Arnaud & Raymond (1992) is largely based on theoretical work by Jacobs et al. (1977) and Hahn (1989). The purpose of this early theoretical work was to produce DR data for modeling coronal equilibrium. However ions form in coronal equilibrium at temperatures about an order of magnitude higher than those where they form in photoionized gas

(Kallman & Bautista 2001). Therefore, it is questionable to use these theoretical DR data for photoabsorption modeling. Benchmarking by experiment is highly desirable.

The only DR measurements for M-shell ions of third- and fourth-row elements available up to now are those for Na-like Fe XVI (Linkemann et al. 1995; Müller 1999); Ar-like Ti V and Sc IV (Schippers et al. 1998, 2002); and Mg-like Ni XVIII (Fogle et al. 2003). Although being of minor astrophysical relevance, the Sc IV and Ti V measurements illustrate that the low-energy recombination spectra of M-shell ions can be dominated by strong resonances associated with $3p \rightarrow 3d$ core excitations.

This work presents the experimental measurement of radiative recombination (RR) + DR for Fe XIV forming Fe XIII. In the temperature range where Fe XIV is expected to exist in a photoionized plasma, our experimentally-derived RR + DR rate coefficient is orders of magnitude larger than the sum of the recommended RR value from Woods, Shull, & Sarazin (1981) and the DR value from the compilation of Arnaud & Raymond (1992). As DR is much larger than RR at these temperatures, this discrepancy is clearly due to errors in the recommended DR data. A similar discrepancy can be expected for the other iron M-shell ions. This has important consequences for the modeling of AGN spectra.

2. EXPERIMENTAL TECHNIQUE

The experiment was performed at the heavy-ion test storage ring TSR of the Max-Planck-Institut für Kernphysik in Heidelberg, Germany (MPI-K). Measurements employed the well established procedures for studying electron-ion recombination. Details of experimental and data reduction procedures as well as further references are given in Schippers et al. (2001, 2004) and Savin et al. (2003).

A beam of ^{56}Fe XIV was provided by the MPI-K accelerator facility. After acceleration to an energy of 4.2 MeV/u the ion beam was injected into the storage ring where it was collinearly overlapped with a magnetically guided electron

¹ Institut für Atom- und Molekülphysik, Justus-Liebig-Universität, Leihgesterner Weg 217, 35392 Gießen, Germany, <http://www.strz.uni-giessen.de/~k3>

² Max-Planck-Institut für Kernphysik, Saupfercheckweg 1, 69117 Heidelberg, Germany, <http://www.mpi-hd.mpg.de/ion-storage/>

³ Gesellschaft für Schwerionenforschung (GSI), Planckstrasse 1, 64291 Darmstadt, Germany, <http://www.gsi.de/>

⁴ Columbia Astrophysics Laboratory, Columbia University, 550 West 120th Street, New York, NY 10027, USA, <http://www.astro.columbia.edu/>

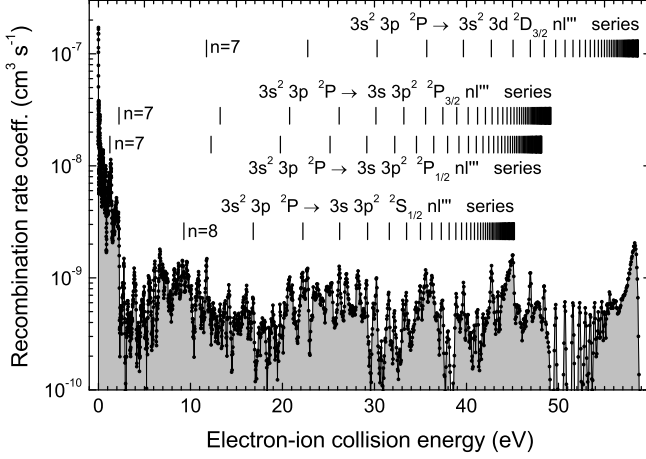


FIG. 1.— Measured Fe XIV to Fe XIII merged-beams electron-ion recombination rate coefficient (MBRRC) in the energy range associated with DR resonances via $3p_{1/2} \rightarrow 3p_{3/2}$, $3s \rightarrow 3p$ and $3p \rightarrow 3d$ core excitations. The vertical bars denote DR resonance positions as expected on the basis of the hydrogenic Rydberg formula. Only the $(3s^2 3d^2 D_{3/2})nl'''$ series of Rydberg resonances can unambiguously be identified. Note that the resonances below 2.3 eV exceed all other resonances in height by an order of magnitude.

beam. In the overlap region the ions can recombine with the electrons via RR and DR. Recombined ions were separated from the ion beam in the first dipole magnet after the electron-ion interaction region and counted using a single-particle scintillation-counter with a nearly 100% detection efficiency. The systematic experimental uncertainty of the measured recombination rate coefficient is estimated to be $\pm 15\%$ (Lampert et al. 1996). This uncertainty stems mostly from the ion current measurement. Adding further uncertainties discussed in Sec. 3 increases this to 18%.

The experimental electron energy distribution is best described as a flattened Maxwellian distribution which is characterized by the longitudinal and transverse temperatures T_{\parallel} and T_{\perp} (see, e. g., Pastuszka et al. 1996). The experimental energy spread $\Delta \hat{E} = [(\ln(2)k_B T_{\perp})^2 + 16 \ln(2) \hat{E} k_B T_{\parallel}]^{1/2}$ depends on the electron-ion collision energy. Here k_B is the Boltzmann constant. In the present experiment the temperatures were $k_B T_{\perp} \approx 12$ meV and $k_B T_{\parallel} \approx 0.09$ meV and consequently $\Delta \hat{E} = 8.3$ meV for $\hat{E} \lesssim 0.2$ eV, $\Delta \hat{E} = 33$ meV at $\hat{E} = 1$ eV and $\Delta \hat{E} = 245$ meV at $\hat{E} = 60$ eV. In the following the experimental data are presented as a merged-beams recombination rate coefficients (MBRRC) $\langle \sigma v \rangle$, i.e., the recombination cross section times the relative velocity convolved with the experimental electron energy distribution.

3. RESULTS AND DISCUSSION

Figure 1 shows the measured Fe XIV MBRRC in the energy range of 0–60 eV. This includes all resonances associated with $3s^2 3p \rightarrow 3s^2 3l'''$ and $3s^2 3p \rightarrow 3s 3p 3l'''$ core excitations. The experimental MBRRC increases strongly at energies below 2.5 eV. Figure 2 shows this energy region in more detail. It is dominated by strong DR resonances that presumably represent levels of the type $(3s 3p^2 \ ^2P_{1/2, 3/2}) 7l'''$. Furthermore the high- l limit of the $(3s 3p^2 \ ^2P_{1/2, 3/2}) 7l'''$ resonances and the series limit of the $3s^2 3p_{3/2} nl'''$ series at 2.337 eV (Behring et al. 1976) are quasi degenerate within ≈ 0.1 eV. DR resonances associated with a $2p^5 \ ^2P_{3/2} \rightarrow \ ^2P_{1/2}$ fine structure excitation were found to be important for low-

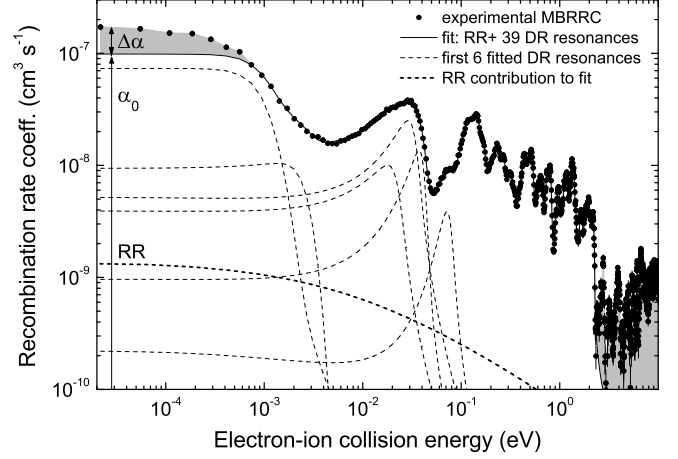


FIG. 2.— Measured Fe XIV to Fe XIII merged-beams recombination rate coefficient (MBRRC) at energies below 10 eV (filled circles). The full curve enclosing the white area is the result of a fit comprising of 39 DR resonances and the contribution from RR (short-dashed curve). The dashed curves show the fits to the first 6 of the 39 DR resonances. The excess rate coefficient $\Delta\alpha$ (see text) contributes to the measured signal at energies below ≈ 1 meV. Here the assumed enhancement factor is $(\Delta\alpha/\alpha_0) + 1 = 1.7$.

temperature DR of Fe XVIII forming Fe XVII (Savin et al. 1997, 1999). The measured Fe XVIII MBRRC exhibits a regular Rydberg series of $(2p^5 \ ^2P_{1/2}) nl'''$ resonances. In the present Fe XIV case such a regular resonance pattern from the $3p_{3/2} nl'''$ series is not observed. The question remains to what extent the unusually strong rise in DR resonance strength below 2.5 eV is caused by the near degeneracy of $(3s 3p^2 \ ^2P_{1/2, 3/2}) 7l'''$ and $3s^2 3p_{3/2} nl'''$ resonances. Accurate theoretical calculations taking into account these features and their mutual coupling through quantum mechanical mixing appear highly desirable in order to understand the detailed electronic dynamics leading to the high resonant rates in this particular energy range.

Up to an energy of ≈ 50 eV the resonance pattern is irregular. Assignment of the observed features could not be achieved with the exception of the $(3s 3p^2 \ ^2S) nl'''$ and $(3s 3p^2 \ ^2P) nl'''$ series limits around 45 and 48 eV, respectively. At higher energies the $(3s^2 3d \ ^2D_{3/2}) nl'''$ Rydberg series is discernable converging to its limit at 58.6722 eV (Behring et al. 1976). This feature was used to calibrate the experimental energy scale. This was achieved by multiplying the experimental energy scale by a factor that deviates from unity by less than 1%.

Finally, Fig. 3 shows the measured Fe XIV MBRRC in the range of 60–260 eV. This range includes resonances associated with $3s \rightarrow 4l''$ and $3p \rightarrow 4l''$ (i.e., $\Delta N = 1$) core excitations. Here N is the principal quantum number of the transitioning core electron. The strongest features in this spectral range are the series limits of the $3p \rightarrow 4l'' nl'''$ resonance series. These occur at about 177.9 eV ($l'' = 0$), 195.0 eV ($l'' = 1$), 210.4 eV ($l'' = 2$), and 221.7 eV ($l'' = 3$) according to the NIST atomic spectra data-base (Ralchenko et al. 2005). Identification of the observed peak features with individual Rydberg series is challenging except for the series limits.

The plasma recombination rate coefficient (PRRC) is derived by convolving the measured MBRRC with a Maxwell-Boltzmann electron energy distribution. As detailed by Schippers et al. (2001, 2004), there are three issues that require special consideration: the experimental energy spread,

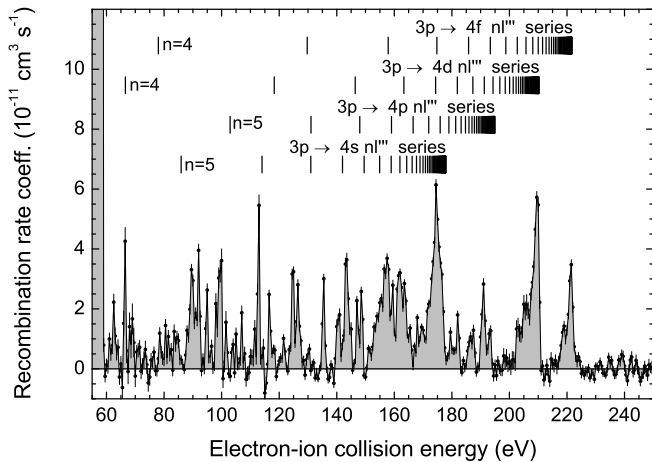


FIG. 3.— Measured Fe XIV to Fe XIII merged-beams recombination rate coefficient in the electron-ion collision-energy region of the $3s^2 4l'' n l'''$ and $3s 3p 4l'' n l'''$ resonances attached to the $3p \rightarrow 4l''$ and $3s \rightarrow 4l''$ core excitations, respectively.

the recombination rate enhancement at low energies, and field ionization of high Rydberg states in the storage-ring bending magnets.

The experimental energy spread $\Delta \hat{E}$ influences the outcome of the convolution for resonances with resonance energies $\hat{E} \lesssim \Delta \hat{E}$. This can be circumvented by extracting the DR cross section from the measured MBRRC at low energies. In Fig. 2 this was achieved by fitting 39 DR resonance line-shapes to the measured spectrum. It should be noted that most probably none of the 39 DR line-shapes correspond to a single resonance but each rather comprises a blend of resonances. Additionally the fit includes a contribution due to RR which was calculated using a semi-empirical hydrogenic formula (Eq. 12 of Schippers et al. 2001).

An enhanced MBRRC is consistently observed in merged electron-ion beam experiments at very low energies. For $\hat{E} \lesssim k_B T_{\parallel}$ the measured MBRRC exceeds the theoretical expectation by factors of typically 2–3 (Gwinner et al. 2000). This excess rate coefficient (labeled $\Delta \alpha$ in Fig. 2) is an artifact of the merged-beams technique and hence a mean excess rate coefficient was subtracted prior to the derivation of the PRRC.

Field ionization of the loosely bound high Rydberg electron in the recombined ions can result from the motional electric fields they experience inside the storage ring bending magnets (Schippers et al. 2001). In the present experiment only RR and DR involving capture into Rydberg levels with quantum numbers less than 55 contribute to the MBRRC.

Similar to the approach of Schippers et al. (2001, 2004) and Fogle et al. (2005), the missing DR resonance strength up to $n_{\max} = 1000$ was estimated from a theoretical calculation using the AUTOSTRUCTURE code (Badnell 1986). Although the AUTOSTRUCTURE code fails to reproduce the irregular Fe XIV resonance structure below 50 eV, it reproduces the more regular resonance structures of high- n Rydberg resonances close to the various series limits reasonably well when slight ‘manual adjustments’ are made to the autoionization transition rates.

The unmeasured DR contribution due to $n > 55$ was estimated to contribute $(15 \pm 7)\%$ to the experimentally-derived Fe XIV PRRC for plasma temperatures $k_B T_e > 9$ eV. The 7%

TABLE 1
PARAMETERS FOR THE FIT OF EQ. 1.

i	c_i ($\text{cm}^3 \text{s}^{-1} \text{K}^{-1}$)	E_i (eV)
1....	3.55E-4	2.19E-2
2....	2.40E-3	1.79E-1
3....	7.83E-3	7.53E-1
4....	1.10E-2	2.21E0
5....	3.30E-2	9.57E0
6....	1.45E-1	3.09E1
7....	8.50E-2	6.37E1
8....	2.59E-2	2.19E2
9....	8.93E-3	1.50E3
10....	9.80E-3	7.86E3

uncertainty was estimated from the adjustment of the transition rates. The same field ionization cut off was taken into account in the RR contribution to the low energy resonance fit in Fig. 2. The unmeasured fraction of the RR-PRRC, due to RR into $3s^2 3p n l$ ($n > 55$) states, was calculated using a hydrogenic formula (Eq. 13 of Schippers et al. 2001, Fig. 4). The RR and DR contributions from $n = 55$ –1000 were subsequently added to the PRRC. The contribution of $\Delta N = 1$ DR with $n > 55$ is insignificant.

For convenient use in astrophysical modeling codes the total Fe XIV to Fe XIII PRRC was fitted using

$$\alpha_{\text{plasma}}(T_e) = T_e^{-3/2} \sum_{i=1}^{10} c_i \exp(-E_i/k_B T_e). \quad (1)$$

The resulting fitting parameters c_i and E_i are given in Table 1. The fit deviates by less than 1% from the experimentally-derived result in the energy range 70 meV–10 keV.

Uncertainties in the non-resonant portion of the background that was not due to RR contributed an estimated 8% error to the measurement. Uncertainties in the exact enhancement factor near 0 eV contributed a 2.1% uncertainty at 0.07 eV, and 1.4% at 0.1 eV, and less than 1% above 0.14 eV. Adding these, the transition rate uncertainty, and the 15% systematic uncertainty in quadrature gives a total experimental uncertainty of $\pm 18\%$ in the energy range 70 meV–10 keV.

4. ASTROPHYSICAL IMPLICATIONS

The approximate temperature ranges where Fe XIV forms in photoionized and in collisionally ionized plasmas can be obtained from the work of Kallman & Bautista (2001). For photoionized plasmas they find that the fractional Fe XIV abundance peaks at a temperature of 4.5 eV. From a different photoionization model, Kraemer, Ferland, & Gabel (2004) obtain a value of 7.8 eV. The ‘photoionized zone’ may be defined as the temperature range where the fractional abundance of a given ion exceeds 10% of its peak value. For Fe XIV this corresponds to a temperature range of 2–14 eV (Kallman & Bautista 2001). Using the same criterion and again the results of Kallman & Bautista (2001), for coronal equilibrium the Fe XIV ‘collisionally ionized zone’ is estimated to extend over a temperature range of 170–580 eV. It should be kept in mind that these temperature ranges are only indicative. In particular, they depend on the accuracy of the underlying atomic data base.

In Fig. 4 we compare our experimentally-derived PRRC with the RR rate coefficient of Woods, Shull, & Sarazin

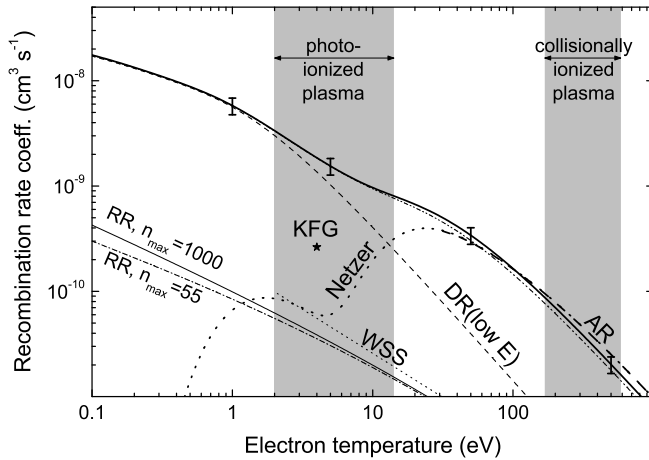


FIG. 4.— Experimentally-derived Fe XIV to Fe XIII recombination rate coefficient in a plasma (PRRC, thick full line) comprising $\Delta N = 0$ DR (Fig. 1), $\Delta N = 1$ DR (Fig. 3), RR, and the theoretical estimate for the unmeasured contributions of states with $n > 55$ for RR and $\Delta N = 0$ DR. The error bars denote the $\pm 18\%$ experimental uncertainty in the absolute rate coefficient. The experimental results without the RR and DR extrapolation are shown by the dash-dot-dotted line. Also shown is the theoretical DR rate coefficient of Arnaud & Raymond (1992, thick dashed line, labeled AR), its deliberate modification by Netzer (2004, dotted line), and the RR calculation by Woods, Shull, & Sarazin (1981, thin dotted line, labeled WSS). The star at 4 eV (labeled KFG) is the estimate of Kraemer, Ferland, & Gabel (2004). The contribution from the low energy DR resonances between 0 and 2.5 eV is shown as the thin dashed line. The curves labeled RR were calculated using a hydrogenic formula (Eq. 13 of Schippers et al. 2001) with $n_{\max} = 1000$ (thin full line) and with $n_{\max} = 55$ (dash-dotted line). The temperature ranges where Fe XIV is expected to peak in abundance in photoionized and collisionally ionized plasmas are highlighted.

(1981) and the recommended DR-PRRC of Arnaud & Raymond (1992). This latter is based on a theoretical calculation by Jacobs et al. (1977) and includes DR associated with $2p \rightarrow 3d$ inner shell transitions. It was calculated for a temperature range of $k_B T = 30\text{--}9000$ eV. In the collisionally ionized zone the experimentally-derived

PRRC is lower than the theoretical result by 21% at $k_B T = 580$ eV. This discrepancy may partly be attributed to the fact that DR resonances associated with $2p \rightarrow 3d$ and higher core excitations were not measured. But given the poor agreement between the calculations of Jacobs et al. (1977) and DR measurements for other iron ions (e.g., Savin et al. 2002), this close agreement is probably fortuitous.

In the photoionized zone the experimentally-derived PRRC is decisively determined by the resonances occurring at electron-ion collision energies below 2.5 eV. The RR contribution is insignificant relative to DR. Our derived PRRC is several orders of magnitude larger than the DR data from the widely used compilation of Arnaud & Raymond (1992). They are still about an order of magnitude larger than the DR-PRRC used by Netzer (2004) and Kraemer, Ferland, & Gabel (2004) who deliberately assumed sets of DR-PRRC for the Fe M-shell ions in order to achieve a better agreement of their plasma modeling results with the observed shape of the Fe $2p \rightarrow 3d$ UTA (cf. introduction).

The present result shows that the previously available theoretical DR-PRRC for Fe XIV forming Fe XIII are much too low, as Netzer et al. (2003) had already suspected. Other storage ring measurements show similar deviations from published recommended low temperature DR-PRRC for M-shell ions (Linkemann et al. 1995; Müller 1999; Fogle et al. 2003). We are now in the process of carrying out DR measurements for other M-shell iron ions. As they become available we recommend that these experimentally-derived PRRC be incorporated into future models of AGN spectra in order to arrive at more reliable results.

We gratefully acknowledge the excellent support by the MPI-K accelerator and TSR crews. This work was supported in part by the German federal research-funding agency DFG under contract no. Schi 378/5. DL, MS, and DWS were supported in part by the NASA Space Astrophysics Research Analysis program, the NASA Astronomy and Astrophysics Research and Analysis program, and the NASA Solar and Heliospheric Physics program.

REFERENCES

- Arnaud, M., & Raymond, J. 1992, *ApJ*, 398, 394
 Badnell, N. R. 1986, *J. Phys. B*, 19, 3827, <http://amdpp.phys.strath.ac.uk/autos/>
 Behar, E., Rasmussen, A. P., Blustin, A. J., Sako, M., Kahn, S. M., Kaastra, J. S., Branduardi-Raymont, G., & Steenbrugge, K. C. 2003, *ApJ*, 598, 232
 Behar, E., Sako, M., & Kahn, S. M. 2001, *ApJ*, 563, 497
 Behring, W. E., Cohen, L., Feldman, U., & Doschek, G. A. 1976, *ApJ*, 203, 521
 Fogle, M., Badnell, N. R., Glans, P., Loch, S. D., Madzunkov, S., Abdel-Naby, S. A., Pindzola, M. S., & Schuch, R. 2005, *A&A*, 442, 757
 Fogle, M., Eklöw, N., Lindroth, E., Mohamed, T., Schuch, R., & Tokman, M. 2003, *J. Phys. B*, 36, 2563
 Gallo, L. C., Boller, T., Brandt, W. N., Fabian, A. C., & Vaughan, S. 2004, *Astron. Astrophys.*, 417, 29
 Gwinner, G., et al. 2000, *Phys. Rev. Lett.*, 84, 4822
 Hahn, Y. 1989, *J. Quant. Spectrosc. Radiat. Transfer*, 41, 315
 Jacobs, V. L., Davis, J., Kepple, P. C., & Blaha, M. 1977, *ApJ*, 211, 650
 Kallman, T., & Bautista, M. 2001, *ApJS*, 133, 221
 Kaspi, S., et al. 2002, *ApJ*, 574, 643
 Kaspi, S., Netzer, H., Chelouche, D., George, I. M., Nandra, K., & Turne, T. J. 2004, *ApJ*, 611, 68
 Kraemer, S. B., Ferland, G. J., & Gabel, J. R. 2004, *ApJ*, 604, 556
 Krongold, Y., Nicastro, F., Elvis, M., Brickhouse, N. S., Mathur, S., & Zezas, A. 2005, *ApJ*, 620, 165
 Lampert, A., Wolf, A., Habs, D., Kenntner, J., Kilgus, G., Schwalm, D., Pindzola, M. S., & Badnell, N. R. 1996, *Phys. Rev. A*, 53, 1413
 Linkemann, J., et al. 1995, *Nucl. Instrum. Methods B*, 98, 154
 Müller, A. 1999, *Int. J. Mass Spectrom.*, 192, 9
 Netzer, H. 2004, *ApJ*, 604, 551
 Netzer, H., et al. 2003, *ApJ*, 599, 933
 Pastuszka, S., et al. 1996, *Nucl. Instrum. Methods A*, 369, 11
 Pounds, K., Reeves, J., O'Brien, P., Page, K., Turner, M., & Nayakshin, S. 2001, *ApJ*, 559, 181
 Pounds, K. A., Reeves, J. N., King, A. R., & Page, K. L. 2004, *MNRAS*, 350, 10
 Ralchenko, Y., Jou, F.-C., Kelleher, D. E., Kramida, A. E., Musgrove, A., Reader, J., Wiese, W. L., & Olsen, K. 2005, NIST Atomic Spectra Database, Version 3.0.2, (Gaithersburg, MD: National Institute of Standards and Technology), <http://physics.nist.gov/asd3>
 Sako, M., et al. 2001, *A&A*, 365, L168
 Savin, D. W., et al. 1997, *Astrophys. J.*, 489, L115
 Savin, D. W., et al. 2003, *ApJS*, 147, 421
 Savin, D. W., et al. 1999, *Astrophys. J. Suppl. Ser.*, 123, 687
 Savin, D. W., et al. 2002, *ApJ*, 576, 1098
 Schippers, S., Bartsch, T., Brandau, C., Gwinner, G., Linkemann, J., Müller, A., Saghir, A. A., & Wolf, A. 1998, *J. Phys. B*, 31, 4873
 Schippers, S., et al. 2002, *Phys. Rev. A*, 65, 042723
 Schippers, S., Müller, A., Gwinner, G., Linkemann, J., Saghir, A. A., & Wolf, A. 2001, *ApJ*, 555, 1027
 Schippers, S., Schnell, M., Brandau, C., Kieslich, S., Müller, A., & Wolf, A. 2004, *A&A*, 421, 1185
 Steenbrugge, K. C., Kaastra, J. S., de Vries, C. P., & Edelson, R. 2003, *A&A*, 402, 477
 Woods, D. T., Shull, J. M., & Sarazin, C. L. 1981, *ApJ*, 249, 399